

Possibility of the Abrasive Wear Resistance Determination with Scratch Tester

A. Vencl · N. Manić · V. Popovic · M. Mrdak

Received: 17 February 2009 / Accepted: 30 November 2009 / Published online: 19 December 2009
© Springer Science+Business Media, LLC 2009

Abstract Abrasion wear resistance is very important in many applications and it is not a surprise that there are many laboratory test methods for its determination. In this article, a possibility of the abrasive wear resistance determination with scratch tester, as a relatively easy and quick test method, was analysed and compared with the standard test method for pin abrasion testing (ASTM G 132). Materials used in the tests were: two ferrous-based coatings (deposited on an Al–Si alloy substrate with atmospheric plasma spraying), two aluminium-based composite materials with 10 wt% of Al₂O₃ reinforcements (produced with compocasting technique) and grey cast iron, known as a material with good abrasive wear resistance. Coefficient of friction and wear of the samples were investigated with both abrasion wear test methods and analysed in correlation with their mechanical properties.

Keywords Abrasive wear · Scratch test · Pin-on-disc test · Coatings · Metal matrix composites

A. Vencl (✉)
Tribology Laboratory, Mechanical Engineering Faculty,
University of Belgrade, 11120 Belgrade, Serbia
e-mail: avenc1@mas.bg.ac.rs

N. Manić
Fuel and Combustion Laboratory, Mechanical Engineering
Faculty, University of Belgrade, 11120 Belgrade, Serbia

V. Popovic
Department of Motor vehicles, Mechanical Engineering Faculty,
University of Belgrade, 11120 Belgrade, Serbia

M. Mrdak
IMTEL Microwaves Inc., 11070 Belgrade, Serbia

1 Introduction

Abrasion wear is one of the most dominant types of wear, and abrasion wear resistance is very important in many applications. Over the 50% of all wear failures are caused by abrasive wear [1]. It is a major problem in the mining and minerals processing industries (bulldozer blades, excavator teeth, drills and chutes, etc.), automotive industry (cylinders, piston rings, clutches and brakes etc.) as well as in other machines that work in contaminated environments (wind turbines, construction and agricultural machinery, etc.). The wear of machine parts, the cost of repair and replacement of these parts, and the associated downtime related to these activities result in significant costs for these industries.

Abrasive wear processes are typically classified as two-body (abrasive particles or protuberances are fixed) and three-body abrasion (abrasive particles are free to slide and/or to roll). Another system of classification divides abrasion into gouging abrasion, high-stress (or grinding) abrasion and low-stress (or scratching) abrasion. In gouging abrasion, large particles are removed from the surface, leaving deep groves and/or pits. The stresses in gouging abrasion are higher than those in high-stress abrasion and are often of a sufficient magnitude to cause generalised plastic deformation of materials. High-stress abrasion is accompanied by the fracture of the abrasive particles and the worn surface may exhibit varying degrees of scratching with plastic flow of sufficiently ductile phases or fracture of brittle phases. Debris may be formed after repeated plastic flow by a fatigue-like mechanism or by chipping. Low-stress abrasion occurs when the load is low enough that the abrasive particles are not fractured and a worn surface usually exhibits fine scratches [2, 3]. Regardless of the classification abrasive wear mechanism could generally be divided into four

types: ploughing, cutting, fatigue and fracture (cracking), resulting with different surface appearance [4].

There are many laboratory test methods for the determination of the abrasive wear resistance. Some of the tests are standardised [5–9] and some are not [10, 11]. All of the laboratory test methods, both standard and non-standard, significance of use are to predict the relative ranking of materials, since the tests do not attempt to duplicate all the conditions that may be experienced in service. One of the non-standard abrasive wear resistance tests is scratch test. Scratch testing is used for many years to evaluate the resistance of materials to scratching damage. The use of scratch testing increased considerably with the application to adhesion testing of coatings [12], and was standardised for that purpose [13]. Since abrasive wear is cumulative action of the scratches produced by a large number of abrasive particles or hard asperities, a single-point scratch test appears to be a logical way to study the material removal process. Scratch test offers a possibility for comparison of different materials relatively easy and in short period of time, with good repeatability. In practice, scratch testing is most often used as a quality control technique enabling the performance of one surface to be qualitatively and, to some extent, quantitatively compared to another which is known to be satisfactory in use [14]. Scratch testing is also a technique that has potential, as a simple test, to provide more fundamental information on wear mechanisms [15–19].

In the scratch test, the load acting between the indenter tip (abrasive particle) and the test sample (worn material) is a very important test parameter, and tests can be broadly divided into two categories. When the load is high, considerable fracture occurs to the material and the abrasive particle, and the wear process is termed high-stress abrasion; when low loads are operating less fracture damage is caused and the wear process is termed low-stress abrasion [20]. In addition to the normal load and other test parameters such as scratch velocity, attack angle (or strain imposed) and temperature, etc. scratching of a material is greatly influenced by the modes of material deformation namely ductile and brittle. It could be expected a drastic change in the material response when there is a change in the material's behaviour from ductile to brittle and vice versa [19].

Aluminium alloys have attractive physical and mechanical properties. They are lightweight, low costs production (with sand casting technology), easy to machine and have good recycling possibilities (up to 95%) (<http://www.eaa.net>). Due to these facts they are often used as a substitution for grey cast iron and steel parts in many industries. Unfortunately, tribological properties of Al-alloys are generally poor comparing with grey cast iron or steel. Coatings as a surface engineering treatment and MMCs are frequently used for improvement of Al-alloys tribological properties.

In this article, the possibility of the abrasive wear resistance determination with scratch tester was analysed and compared with the standard test method for pin abrasion testing (ASTM G 132). Materials used in the tests were: two ferrous-based coatings (deposited on an Al–Si alloy substrate with atmospheric plasma spraying), two aluminium-based composite materials with 10 wt% Al_2O_3 reinforcements (produced with compocasting technique) and grey cast iron, known as a material with good abrasive wear resistance. Coefficient of friction and wear of the samples were investigated with both abrasion wear resistance test methods and analysed in correlation with their mechanical properties.

2 Experimental

2.1 Materials

Substrate material for the coatings deposition was an Al–Si alloy (EN AlSi10Mg) with following chemical composition: Al–9.8Si–0.48Fe–0.1Cu–0.2Mn–0.3 Mg–0.08Zn–0.05Ti (wt%) and it was produced using sand casting, followed with solution annealing at 540°C with 35°C/h, water quenching and artificial ageing at $160 \pm 5^\circ\text{C}$ for 6 h. Two spray powders were used in the experiment: ‘Metco 92F’ and ‘Sulzer Metco 4052’, which are commercial brand names of Metco Inc. and Sulzer Metco Inc., respectively. The chemical compositions of the *Metco 92F* powder was: Fe–3.5C–0.35Mn (wt%) and the chemical compositions of the *Sulzer Metco 4052* was: Fe–1.2C–1.5Mn–1.3Cr–0.3Ni (wt%). The powders particle granulations were: $-53/+10 \mu\text{m}$ (*Metco 92F*) and $-38/+15 \mu\text{m}$ (*Sulzer Metco 4052*). For the convenience, the coatings attained using *Metco 92F* and *Sulzer Metco 4052* powders are hereafter referred to as 92F and 4052, respectively. Coatings deposition was done with Atmospheric Plasma Spraying (APS). Before the spraying process, surface of the substrate was activated with brown-fused alumina (Al_2O_3) using particle sizes of 106–125 μm . The target coating thickness was 200–300 μm . Details of the technology process and spray conditions are described elsewhere [21].

The matrix material of the composites was an Al–Si alloy (EN AlSi7Mg0.3) with the following chemical composition: Al–7.2Si–0.02Cu–0.29 Mg–0.01Mn–0.18Fe–0.01Zn–0.02Ni–0.11Ti (wt%). Composites were produced by the compocasting technique using mechanical mixing of the matrix, i.e. Al_2O_3 particles as reinforcement were added into the semi-solid Al–Si alloy by infiltration and admixing. The amount of particles was 10 wt%, whereas the average size of Al_2O_3 particles was 12 μm and 35 μm (hereafter referred to as 10-12 and 10-35, respectively). Experimental procedure and apparatus used for the compocasting

processing are described and discussed elsewhere [22]. Composite specimens were subjected to heat treatment with following parameters: solution annealing at 540°C for 6 h, water quenching and artificial aging at 160°C for 6 h.

A grey cast iron (hereafter referred to as SL 26) was chosen as a standard material to compare its performances with the above-mentioned two coatings and two composites. The chemical composition of grey cast iron, fabricated using the sand casting procedure followed with heating at 550°C to eliminate residual stress in the material, was: Fe–3.18C–2.17Si–0.60Mn–0.7P–0.37Cr (wt%).

2.2 Structural and Mechanical Examinations

The microstructure of test materials was analysed by optical microscope (OM), where the coatings were sectioned perpendicular to the coated surface. Metallographic samples of matrix material and composites were prepared in a standard way applying grinding and polishing, whereas etching in Keller's solution (the mixture of 95 ml H₂O, 2.5 ml HNO₃, 1.5 ml HCl and 1 ml HF) was used to reveal the microstructure of materials.

Phases that were present in the coatings were analysed by the X-ray diffraction (XRD). After an identification of oxides and their volume fraction, porosity and presence of cracks and unmelted particles their percentage share was measured by image analysis on OM micrographs. Characterisation of the coatings was done according to the Pratt and Whitney standard [23].

Tensile bond strength tests on the coatings were performed on a hydraulic tensile test rig using a crosshead velocity of 0.5 mm/min. The bond strength was calculated by dividing the maximum (failure) load by the cross-sectional area of the specimen. The geometry of the specimens was according to the ASTM C633 standard [24]. Two specimens in pair were used, and the coating was deposited only on one of them. Specimens were bonded by glue and kept pressed against each other in a furnace at a temperature of 180°C for 2 h. The presented results of the coating's tensile bond strength testing represent an average value of a larger number of tests.

Microhardness measurements were carried out using a 1368 Vickers diamond pyramid indenter and 100 g load. At least six measurements were made for each specimen to eliminate possible segregation effects and to get a representative value of the material microhardness. Density of the specimens was measured by Archimedes method.

2.3 Tribological Testing

Scratch abrasion wear tests were carried out on the scratch tester under dry sliding conditions, in ambient air at room temperature ($\approx 25^\circ\text{C}$). Stylus (indenter) was pressed with

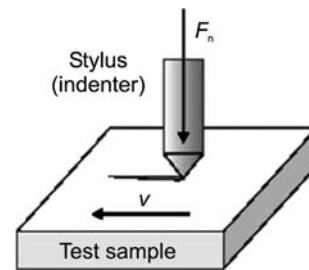


Fig. 1 Schematic diagram of scratch tester

selected normal load against test sample and moved with constant velocity, producing the scratch of certain width and shape on the test sample. Surface roughness of test samples was around $R_a = 0.5 \mu\text{m}$. A schematic diagram of scratch tester is presented in Fig. 1.

Indenter cone was diamond with radius of 0.2 mm. The indenter velocity of 10 mm/min was used over a wear tracks of 10 mm, with different normal loads applied. Composites, as relatively soft materials, showed very low abrasion wear resistance, and for their testing applied normal loads were lower than for the other tested materials. For all materials, two modes of scratch testing were used: PLST (Progressive Loading Scratch Test) and CLST (Constant Load Scratch Test) [13]. In PLST mode, the normal load was increased linearly during the test from 0 to 100 N (for SL 26 and coatings) and from 0 to 50 N (for composite materials). In CLST mode, the normal load was constant during the test and was increased step by step between the tests: 20, 40, 60, 80 and 100 N (for SL 26 and coatings) and 10, 20, 30, 40 and 50 N (for composite materials). From each material, in both PLST and CLST mode, two samples were chosen and three scratches were made on each sample, maintaining a gap of at least 1 mm in between two scratches.

Before and after testing, both the indenter and the test samples were degreased and cleaned with benzene. Wear scars on test samples were measured on Surface Roughness Measurement System 'Talysurf 6', after each CLST mode test to calculate the volume loss. Volume loss was calculated from the cross-sectional area of displaced material (Fig. 2) multiplied by the wear track length. Displaced material area was chosen because it is assumed that, since a

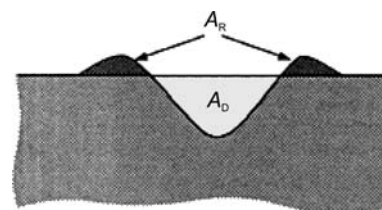


Fig. 2 Cross-sectional areas perpendicular to a wear scar on an initially flat surface (A_D —cross-sectional area of displaced material and A_R —cross-sectional area of formed ridges)

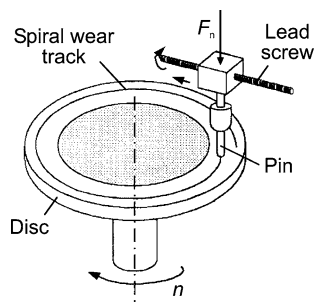


Fig. 3 Schematic diagram of pin-on-disc tribometer

single-pass scratching is performed, the ability of the ridges to withstand deformation from a subsequent scratching would not be enough and that the ridges would be removed. The values of friction coefficient, normal and friction force were monitored during the test and through data acquisition system stored in the PC. After testing, worn surfaces of test samples were examined by Scanning Electron Microscope (SEM).

Pin-on-disc abrasion wear tests were carried out on the pin-on-disc tribometer according to the standard test method for pin abrasion testing (ASTM G 132), in ambient air at room temperature ($\approx 25^\circ\text{C}$). The end of a pin, which was not rotating about its axis, was positioned perpendicular to the alumina-coated abrasive paper with grain size of $46.2\ \mu\text{m}$ (P320 grit), which was supported by a flat horizontal rotating disc (100 mm in diameter, 20 r.p.m.). Cylindrical pin (test sample), 2.5 mm in diameter and 30 mm long, was pressed by dead weights loading system and progressively moved over unused abrasive in a continuous, non-overlapping spiral path in the same way as in lapping. Surface roughness of pins was around $R_a = 0.5\ \mu\text{m}$. A schematic diagram of pin-on-disc tribometer is presented in Fig. 3.

Testing was performed under normal load of 1.83 N, i.e. under specific normal load—pressure of 0.37 MPa (taking into account the contact area of approximately $5\ \text{mm}^2$). Sliding distance of 5 m was constant, with an average sliding velocity of 0.072 m/s calculated from the distance/time ratio. The testing parameters were chosen to provide a

reasonable amount of wear, i.e. at least 1 mg loss. For each material, to achieve a higher confidence level in evaluating test results, at least four runs were performed and the results averaged.

Before and after testing, pins were degreased and cleaned with benzene. Pins were weighed with accuracy of $10^{-4}\ \text{g}$ before and after each test to calculate the mass loss. Mass loss values were converted to volume losses using the measured values of test sample densities. The value of friction force was monitored during the test and through data acquisition system stored in the PC, enabling the calculation of friction coefficient. After testing, worn surfaces of pins were examined by SEM.

3 Results and Discussion

3.1 Microstructures

Microstructure of the grey cast iron (SL 26), which was a referent material, consists of phosphide eutectic and graphite flakes in the fine pearlite matrix, as shown in Fig. 4a. A graphite flakes, No. 4–6 in size, conformed to the type A and B morphologies.

The microstructures of two investigated coatings are shown in Figs. 4b and c. In boat coatings, elongated splats of molten powder form a curved lamellar structure, with oxide layers in between, which is typical for spray coatings [24–27]. No cracking was found in the coatings and no peeling was observed at the interface between the coating and the substrate. The distribution of coating thicknesses can be regarded as very stable. Oxide content for coating 92F was approximately 13% and porosity was 2.3%. Presence of unmelted particles and precipitates was not detected in coating 92F. Oxide content for coating 4052 was around 41% and porosity was 5.8%, with bigger pores of irregular shape. It must be mentioned that porosity of the coating 4052 was detected in areas with unmelted particles. Volume fraction of unmelted particles and precipitates in the coating 4052 was approximately 10%.

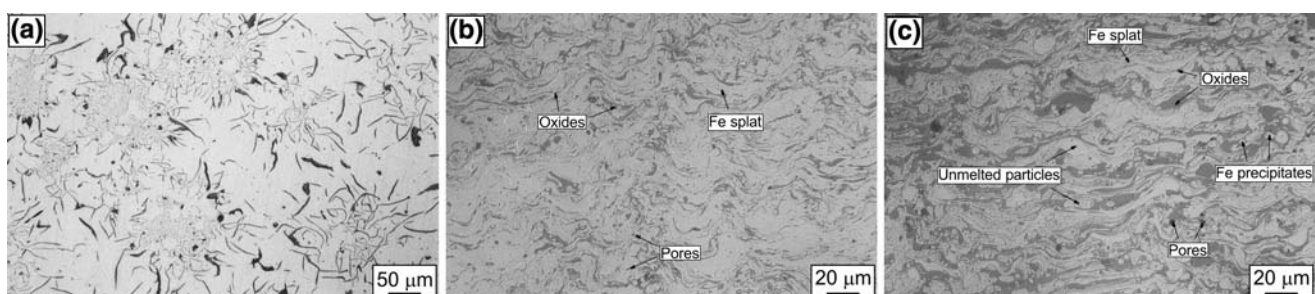


Fig. 4 Microstructures of: **a** SL 26 material, **b** coating 92F and **c** coating 4052

X-ray diffraction (XRD) analysis revealed that coating 92F structure consists of elemental iron (Fe) and magnetite (Fe_3O_4), while coating 4052 contains elemental iron (Fe) and wustite (FeO). Other phases are present in a small amount, less than 3%.

The results of metallographic investigation of the matrix alloy and composites are illustrated in Fig. 5. The microstructure of the matrix alloy consists of fully dendritic primary α phase and a eutectic in interdendritic area (Fig. 5a). Microstructure of composites (Fig. 5b, c) suggests that during the compocasting a transformation from a typical dendritic to a non-dendritic structure of the primary α phase occurred as a result of shear forces generated by the mixer rotation, i.e. the microstructure of composites is distinguished by large primary α phase rosettes. Significant coarsening of the α phase occurred during compocasting. Reinforcement of Al_2O_3 particles are visible not only in the eutectic zone, they are also infiltrated in the α phase primary particles. Infiltration of reinforcement particles into the primary α phase which appear below the liquidus temperature and during mixing is obviously the result of collisions and interactions of the α phase and Al_2O_3 particles. The remainder of the reinforcement was pushed to the eutectic zone consisting of α phase, rod-like silicon particles and Al_2O_3 particles mixture (Fig. 5c). In the microstructure of the composite 10-12, formation of the Al_2O_3 particle agglomerations (with lot of particle-to-particle boundary surfaces) was present. This type of agglomeration reduces the values of the mechanical characteristics. Smaller reinforcement particles, that generally have higher tendency for bonding and agglomeration, did not spread homogeneously into the matrix (Fig. 5b). The size and the shape of the separated silicon particles in composites eutectic determine the morphology of eutectic which has a great effect on the mechanical properties of the material.

3.2 Physical and Mechanical Properties

Coating thickness before machining was 200 and 270 μm for coating 92F and 4052, respectively. With machining, 100 μm of coating thickness was removed.

The obtained value of the tensile bond strength (Table 1) of coating 92F with the substrate of 31.08 MPa was higher than the prescribed value (20.68 MPa) [28]. The value of the tensile bond strength of coating 4052 with the substrate of 32.91 MPa was lower than the expected value (40 to 50 MPa), but still higher than the minimum prescribed value (30 MPa) [29]. For both coatings, the fracture during the testing, occurred through the coating layers near the coating/substrate interface. The values of tensile bond strength depend strongly on the surface roughness, sprayed material, spray parameters, used plasma gun and coating thickness. The obtained lower value of tensile bond strength of the coating 92F with the substrate also indicates weaker cohesion strength of sublayers.

Microhardness and density values of reference material (SL 26), coatings 92F and 4052, composites 10-12 and 10-35, as well as matrix material are shown in Table 1. The microhardness of coatings is affected by the hardness of the coating matrix and oxides, and by the volume porosity. Microhardness of both coatings was in the expected limits: for coating 92F (500 to 700 HV 0.3) [28] and for coating 4052 (350 to 650 HV 0.3) [29]. The coating 92F shows the higher value of microhardness than the coating 4052 because it has denser layers (with less porosity), and has better cohesion of sublayers. Compared to coating 92F, coating 4052 contains bigger pores and higher contribution of porosity, spherical Fe precipitates and unmelted particles. Microhardness and density of the composites increase with addition of Al_2O_3 particles, comparing to the matrix material. Apart from the reinforcing effect of Al_2O_3 particles, the increase of hardness with aging (part of the applied heat treatment) is a result of the precipitation of fine β' particles (Mg_2Si) or S-phase (Al_2CuMg) [30]. Lower than expected values of the composite 10-12 microhardness are in correlation with its microstructure and formation of the agglomerations with lot of particle-to-particle boundary surfaces.

3.3 Scratch Testing

The results of the scratch testing indicate good repeatability of the wear and friction results. Average standard

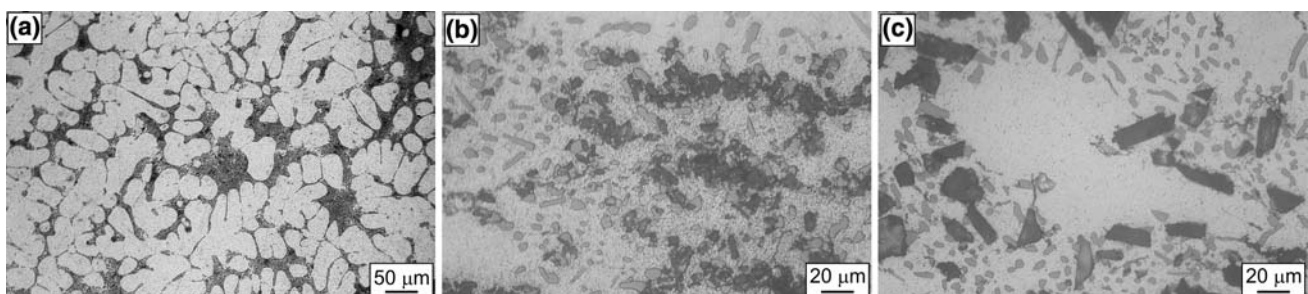


Fig. 5 Microstructures of the heat treated and etched specimens of: **a** matrix alloy, **b** composite 10-12 and **c** composite 10-35

Table 1 Physical and mechanical properties of tested materials

Properties	Material					
	SL 26	Coating 92F	Coating 4052	Matrix material	Composite 10-12	Composite 10-35
Tensile bond strength (MPa)	–	31.08	32.91	–	–	–
Hardness (HV 0.1)	329	495	390	66	73	107
Density (g/cm ³)	7.22	5.52	6.67	2.62	2.66	2.71

deviations (for five different normal loads) of the scratch width were: 9.17% (SL 26), 8.91% (coating 92F), 9.61% (coating 4052), 9.94% (composite 10-12) and 9.52% (composite 10-35).

Wear volumes were calculated from wear scars' profiles, at the end of CLST mode tests. Some of the scars' profiles are shown in Fig. 6. Plastic deformation and formation of the ridges at the scar edges for the SL 26 and both coatings were noticed only at higher normal loads, while for the both composite materials plastic deformation and formation of the ridges at the scar edges were noticed even at lowest applied normal load of 10 N (Fig. 6c).

Wear rates of tested materials, calculated from the volume of the scratch and divided by the length of the scratch, as functions of normal load are shown in Fig. 7. Tendency for all materials was the same: wear rate increases with increase of normal load. For composite materials, this increase of wear rate with increase of normal load was linear function while for SL 26 and both coatings it was exponential growth function. This exponential

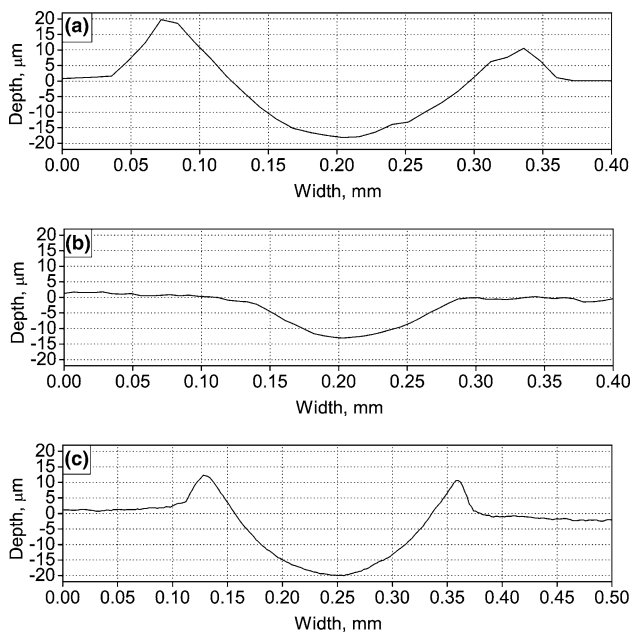


Fig. 6 Wear scars profiles of: **a** SL 26 for normal load of 60 N, **b** coating 92F for normal load of 60 N and **c** composite 10-12 for normal load of 10 N

growth indicates the change of the dominant type of abrasive wear. Wear rates of the both composites, for the same normal load, were one order of magnitude higher than the wear rate of SL 26, while both coatings had lower wear rates than SL 26. Between two composites, 10-35 showed lower values of wear rate (Fig. 7b). This is principally due to the fact that composite 10-35 is harder than composite 10-12, but also because it has larger size of reinforcement particles. Zhang et al. [18] found that particle size and ratio of the penetration depth to particle size are very important parameters. When the particles are relatively large i.e. when the ratio of the penetration depth to particle size is less than unity, materials are difficult to be removed by the indenter, but if it is larger than unity, materials tend to be removed more easily. Comparing the tested materials by the abrasive wear resistance it could be concluded that both coatings could be an adequate substitution for grey cast iron while both composites could not be a satisfactory substitution.

Dependence of friction force on normal load in PLST mode, for all tested materials, is shown in Fig. 8. If we compare SL 26 and coatings 92F and 4052, the values of friction forces were lowest for coating 4052 followed with coating 92F and SL 26, with highest values. Appearance of the curves was straighter at lower loads than at higher loads, where oscillation of friction force occurred with changing of the curve slopes. This also indicates the change of dominant type of abrasive wear and type of deformation under and ahead the indenter. For SL 26, change of the curve slope was relatively early, comparing to coatings 92F and 4052. For both composite materials, the values of friction forces were lower than for the other tested materials, and changing of the curves' slopes occurred at very low normal loads. Between two composites, 10-12 showed lower values of friction force.

For material SL 26, plastic flow of the material and formation of the micro-chips at the scar edges, typical for ploughing mechanism, was noticed (Fig. 9a). For both coatings, this plastic flow of the material was not noticed in a significant metre, which is in correlation with the fact that both coatings had lower ductility than SL 26. On both coatings, the base lamellar structure of the coatings is still visible. Predominant features were formation of transverse cracks and brittle fracture (Fig. 9b, c). Delamination of the

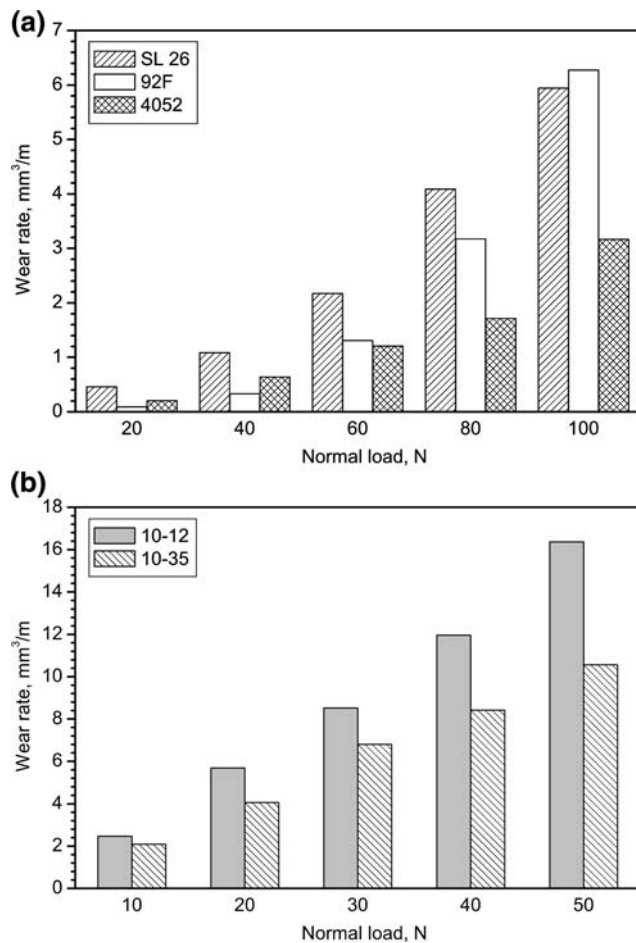


Fig. 7 Wear rates of tested materials for different normal loads: **a** SL 26 and coatings 92F and 4052 and **b** composites 10-12 and 10-35

fragments, characteristic for fracture (cracking) mechanism, from coating 4052 can be attributed to the higher presence of oxides, noticed during the microstructure analysis, comparing to coating 92F. The cracks on the worn surfaces appeared on the oxides/matrix interfaces, as well as through the oxides, leading to the separation of the whole parts of the coating (Fig. 9d). High presence of pores in coating 4052 additionally affected creation of the cracks and detachment of the coatings fragments. Big and irregularly shaped pores make less favourable microstructure of thermally sprayed coatings because they are a source of residual stresses and have an influence on creating of cracks [31]. They also decrease the hardness and bond strength between coating layers. For both composite materials, ploughing was dominant type of abrasive wear. Formations of transverse cracks were significantly less pronounced than for both coatings. Plastic deformation and intensively extrude of the material at the scar edges were noticed even at low normal loads (Fig. 9e, f).

Values of the coefficient of friction, from CLST mode, for all tested materials increase with increase of normal

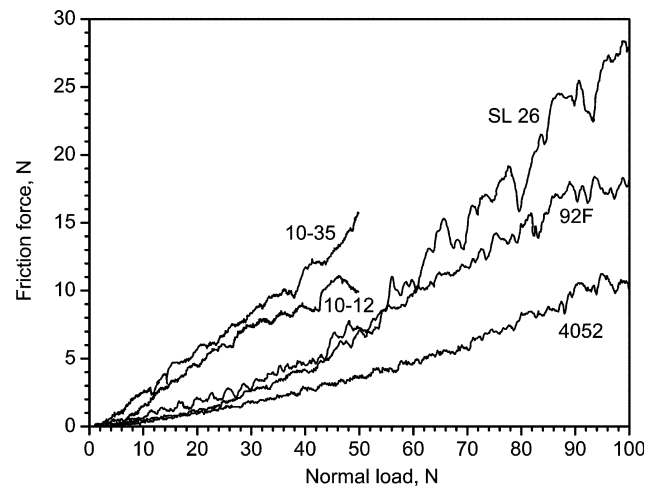


Fig. 8 Friction force versus normal load for tested materials in PLST mode

load, but after some value of normal load they show tendency for stabilization. These mean values (after stabilization) of coefficient of friction are shown in Table 2.

For both coatings, values of the coefficient of friction were lower than for SL 26, principally because of their higher hardness. Attained coefficient of friction values of the grey cast iron and both coatings were in expected range for metals and plasma sprayed coatings in scratch testing conditions [15, 16, 20]. For composite materials, presence of the reinforcement particles had small influence on wear rate as well as on friction coefficient. Values of the friction coefficient for composites were lower than it is expected in scratch testing conditions [18] and controlled principally by the hardness and other characteristics of the matrix material.

3.4 Pin-on-Disc Testing

The repeatability of the results in pin-on-disc testing was as follows: 7.73% (SL 26), 5.05% (coating 92F), 7.46% (coating 4052), 12.22% (composite 10-12) and 11.35% (composite 10-35) standard deviation of the wear volume.

Obtained results of the wear rates and coefficients of friction, for tested materials, are shown in Table 3. If we compare coatings and SL 26, the highest wear rates had coating 4052, then SL 26 and at the end coating 92F. Intensive wear of the coating 4052 compared with the coating 92F can be explained with higher porosity in this coating. High presence of oxides in the coatings had influence on their wear values. Oxides are harder than Fe splats (matrix) and when the difference is too large, cracks are initiated at oxides and at oxides/matrix interfaces (pre-existing pores and cracks play a similar role), and parts of oxides are fallen off as wear proceeds, causing large protruberances on the worn surface [25, 32]. Low fracture

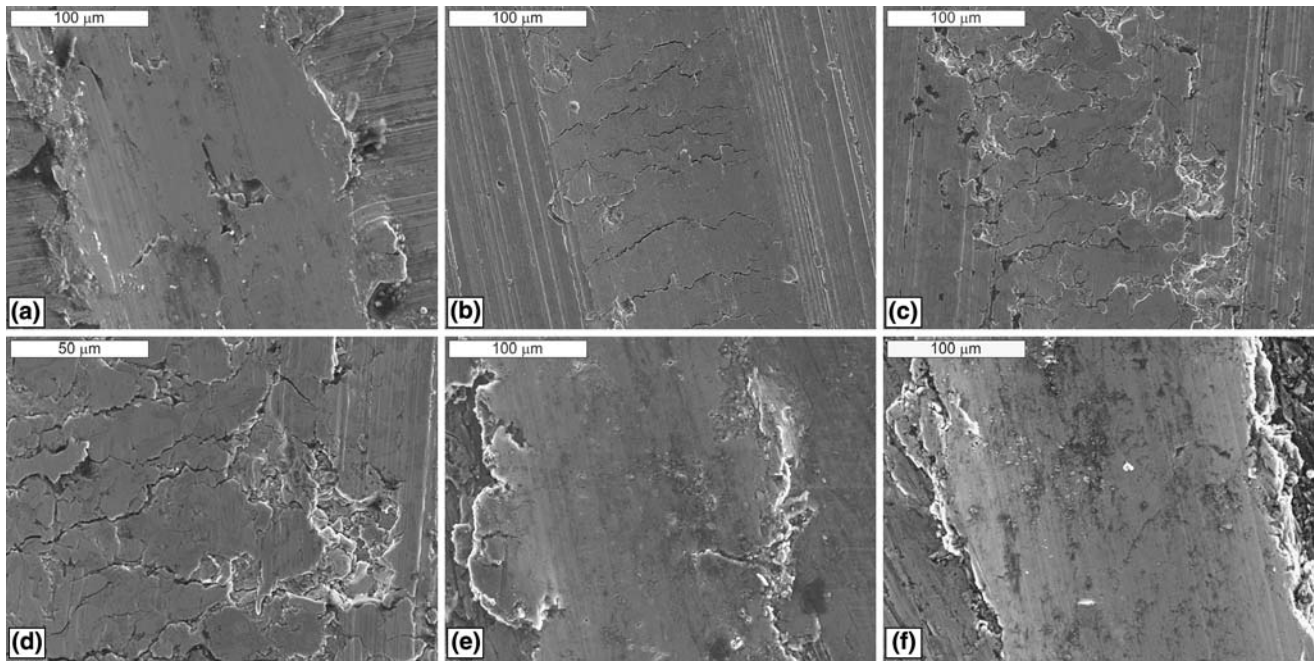


Fig. 9 Wear scar appearance (SEM) of: **a** SL 26, **b** coating 92F, **c** and **d** coating 4052, **e** composite 10-12 and **f** composite 10-35 (wear scar of SL 26 and coatings 92F and 4052 were under the normal load

of 60 N while wear scar of composites 10-12 and 10-35 were under the normal load of 10 N)

Table 2 Coefficient of friction means values of tested materials for scratch testing

Material	SL 26	Coating 92F	Coating 4052	Composite 10-12	Composite 10-35
Value	0.28	0.18	0.11	0.23	0.27

toughness of the interfacial oxide could also cause splat delamination upon frictional contact [33]. It is possible that unmelted particles and precipitates were also fallen off and have caused heavier wear of coating 4052 than coating 92F, since it was present more in coating 4052. For SL 26, wear values should not be viewed only as a function of hardness, yet a presence of graphite as a solid lubricant should also be considered.

Wear rates of both composites were significantly higher than the wear rate of SL 26. Similar to the scratch testing results, composite 10-35 showed lower values of wear rate than composite 10-12. Composite 10-35 is harder than composite 10-12, but also it has larger reinforcement particles. García-Cordovilla et al. [34] showed that the

composites with smaller reinforcement particles exhibit lower abrasive wear resistance. Since the matrix/particles' interfacial area, for the same content of particles, decreases as the size of the particles increases, large particles remain embedded longer than small particulates, until the matrix can no longer support them or until they are broken down into smaller pieces.

Comparing the tested materials by the abrasive wear resistance it can be concluded that, as well as in scratch testing, both coatings can be an adequate substitution for grey cast iron while both composites can not be a satisfactory substitution.

SEM micrographs of tested materials worn surfaces are shown in Fig. 10. Abrasive wear grooves and scratches

Table 3 Wear rates and coefficient of friction means values of tested materials for pin-on-disc testing

Properties	Material				
	SL 26	Coating 92F	Coating 4052	Composite 10-12	Composite 10-35
Wear rate ($\text{mm}^3/\text{m} \times 10^{-2}$)	4.67	4.11	8.89	28.41	21.52
Coefficient of friction	0.50	0.49	0.48	0.73	0.67

were noticed on all tested samples. The general morphological features of the SL 26 and both coatings abraded surfaces are similar to those observed in the early stages of metallographical specimen preparation. Basic lamellar structure of the grey cast iron is still visible (Fig. 10a). Presence of voids from the detached oxides, unmelted particles and precipitates and ‘opened’ pores was also noticed on the worn surfaces of both coatings. Higher presence of these voids in coating 4052 comparing to coating 92F is obvious (Fig. 10b, c).

On the abraded surfaces of composites (Fig. 10d, e), plastic flow of material was noticed, as well as sporadic deep caverns formed by the pull outs of Al_2O_3 particles from the matrix (denoted by arrow in Fig. 10f). These caverns indicate relatively weak interfacial bonding between aluminium matrix and Al_2O_3 particles in these areas. Dominant type of abrasive wear mechanism was ploughing followed with fatigue. Al-Rubaie [35] showed that the dimensions of the abrasive particle relative to the size of the reinforcement determined whether the wearing composite act as a heterogeneous or homogeneous solid. For abrasive particle, and consequently grooves, much larger than the reinforcing phase, the material will be grooved similarly to a homogeneous material which means the interaction between abrasives and reinforcing phase will be of less importance. If the reinforcing particles are comparable in size with the scale of the abrasion damage, or larger, then the material will respond heterogeneously. Similar influence of the reinforcement size on the worn surfaces appearance occurs for tested composite materials.

Since the reinforcement particle size (12 and 35 μm for composites 10-12 and 10-35, respectively) was smaller than abrasive grain size (46 μm) both materials responded similarly to a homogeneous material, i.e. matrix material.

Attained friction coefficient values of tested materials were in expected range for metals in dry sliding conditions (Table 3). Moreover, the relations between the different materials were the same as for the same samples subjected to dry sliding adhesive wear at room temperature [36, 37]. Grey cast iron (SL 26) and coatings showed very similar values, while composites had higher values of the coefficient of friction than SL 26, principally due to the presence of hard reinforcing particles.

4 Correlations of Wear and Friction Data

Five different materials (grey cast iron, two ferrous-based coatings and two aluminium-based composites with Al_2O_3 reinforcements) were investigated using the scratch test and pin-on-disc test, to determine their abrasive wear behaviour. Alongside with the determining of the wear behaviour of these materials an idea was to investigate the possibility of the abrasive wear resistance determination with scratch tester, by comparing it with the standard pin-on-disc abrasion test method.

The scratch tester simulates two-body, gouging or high-stress (depending on the normal load) abrasive wear. It is a relatively easy and quick test method. An advantage over the pin-on-disc test method is that it can simulate very high

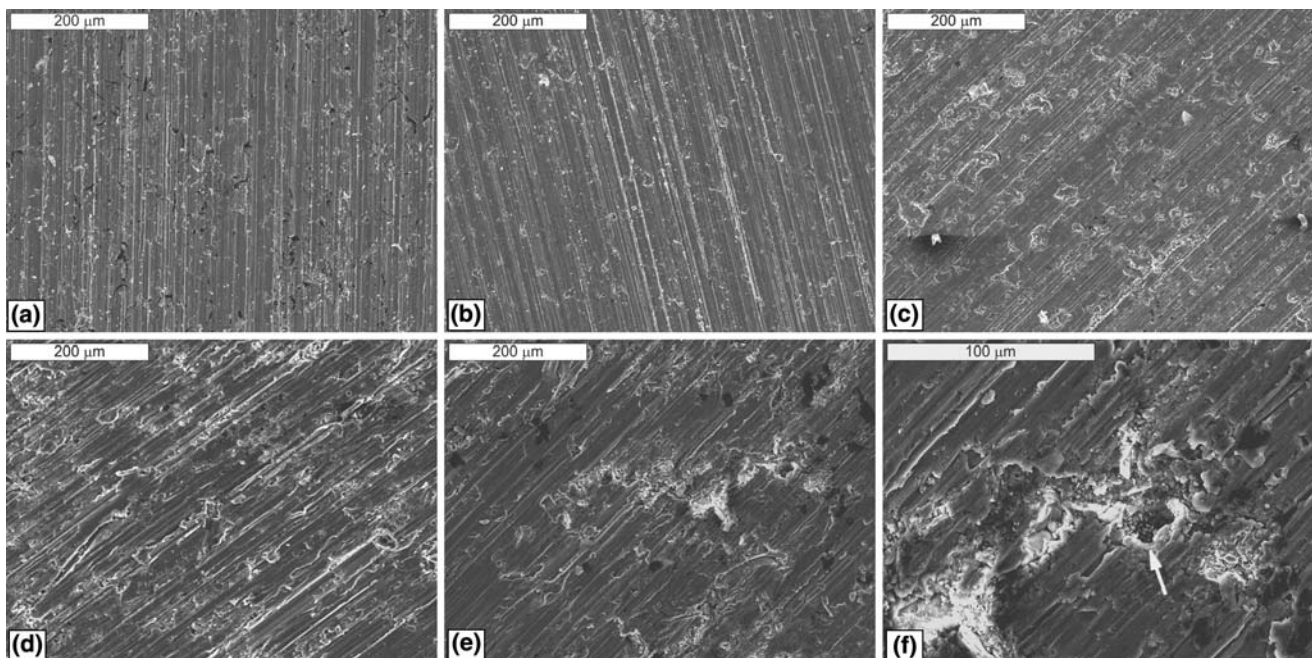


Fig. 10 SEM micrographs of the pins worn surfaces: **a** SL 26, **b** coating 92F, **c** Coating 4052, **d** composite 10-12 and **e** and **f** composite 10-35

loads due to the indenter geometry and the construction of the apparatus. The pin-on-disc abrasive wear test involves two-body and high-stress abrasive wear. This test is classified as high-stress on the grounds that the abrasive particles are sharp, and effectively 'remain' sharp, since as mentioned earlier, these tests stipulate that the specimen always traverses unused areas of abrasive paper. Having sharp abrasive makes the test similar to high-stress abrasion, where particle fracture generates fresh sharp cutting edges. In our case, abrasives were not fractured to any substantial degree during the testing. Both tests showed good repeatability of the results, with the standard deviation less than 10% (except for the composites in pin-on-disc test).

In addition to the wear and friction data, the hardness of each of tested materials was determined, as an ancillary mechanical property, to make appropriate correlations. It is well known that hardness of commercially pure metals influences its abrasive wear resistance and that higher hardness implies a higher wear resistance. Khrushov [38] finds out that increase of the wear resistance depends on the way in which the metal is being hardened (alloying, heat treatment or work-hardening) and that in some cases wear resistance decreases with increase of hardness. The same author establishes a correlation between the abrasive wear resistance and Young's modulus, and shows that wear resistance increases with increase of material Young's modulus [39]. The results of other researchers also show that abrasion wear resistance of quenched and tempered steels has a much weaker dependency on bulk hardness [40].

The use of hardness as a parameter for predicting the wear behaviour of materials must be done with caution. For instance wear mechanisms of thermal spray coatings represent a more complex form of wear processes due to their lamellar structure. Higher wear resistance of these coatings can be achieved by increasing their hardness, up to a certain level, through forming of an appropriate amount of oxides, but high hardness difference between matrix and oxides can also induce higher wear [25, 32]. For the aluminium-based composites, Straffelini et al. [41] for instance found that the matrix hardness exerts a much stronger influence on the dry sliding wear behaviour of Al_2O_3 particles reinforced composite than bulk hardness, and that the composite with the lowest matrix hardness displays the lowest wear rate.

The relationships between obtained values of the wear rate and coefficient of friction with the hardness of tested materials are shown in Figs. 13 and 14, for scratch testing and for pin-on-disc testing, respectively.

The first feature is the general relationship of the abrasive wear rate decreasing with hardness for both abrasion testing. This relationship was not linear in neither of the

tests. As with most generalities there are exceptions. One of the exceptions in scratch testing was the performance of coating 92F, for higher loads (60, 80 and 100 N). This coating as the material with the highest hardness did not show, for the mentioned higher loads, the lowest wear rates (Fig. 11a). The same trend was also observed between coefficient of friction and sample hardness of coating 92F, i.e. for the higher loads (60, 80 and 100 N), there was no clear variation in final coefficient of friction with sample hardness (Fig. 11b). The opposite behaviour of the hard coatings was noticed by Gee [20]. He showed that for the high loads' scratch testing (50 N), there is a strong correlation between scratch width (abrasion resistance) and hardness of the sample, while there is very little if any correlation between the abrasion resistance and the sample hardness for the low loads scratch testing (4 N). There is no simple explanation for this behaviour of coating 92F. It could be due to the fact that coating 92F had weaker cohesion strength of sublayers and that it is more ductile than coating 4052 but most probably the reason for coating 92F behaviour at very high load is connected with the microstructure of the coating. Attained relationships of the wear rates and coefficients of friction with sample hardness indicate that different behaviour of the materials can be expected for very high load scratch testing (above 50 N). In the pin-on-disc testing, coating 4052 performed worse than expected (with respect to its pre-test hardness), and 92F to some extent (Fig. 12). This is probably because coating 4052 was less homogeneous in nature, than coating 92F and especially than SL 26, as it was noticed in the microstructure analysis.

The results of the abrasive wear performance of the composites investigated in this study indicate that a general trend is valid, namely, a higher hardness is usually associated to a better resistance to abrasion and lower coefficient of friction. The coefficient of friction values in scratch testing was an exception, as in these testing the average friction coefficient of two composites increases with increase of hardness (Fig. 11b). Similar behaviour of aluminium matrix composites in single scratch tests was also noticed by Zhang et al. [18]. Relatively high values of wear rate of composites are due to the fact that the high loads were applied and the reinforcement particles were unable to protect the soft Al–Si alloy matrix from wear.

Wear rates of all tested materials were more than one order of magnitude higher in scratch testing than in pin-on-disc testing, while coefficients of friction were more than twice less in scratch testing than in pin-on-disc testing. This is principally because of the different contact geometry between the abrasives and tested samples and due to the fact that in scratch testing significantly higher loads were applied.

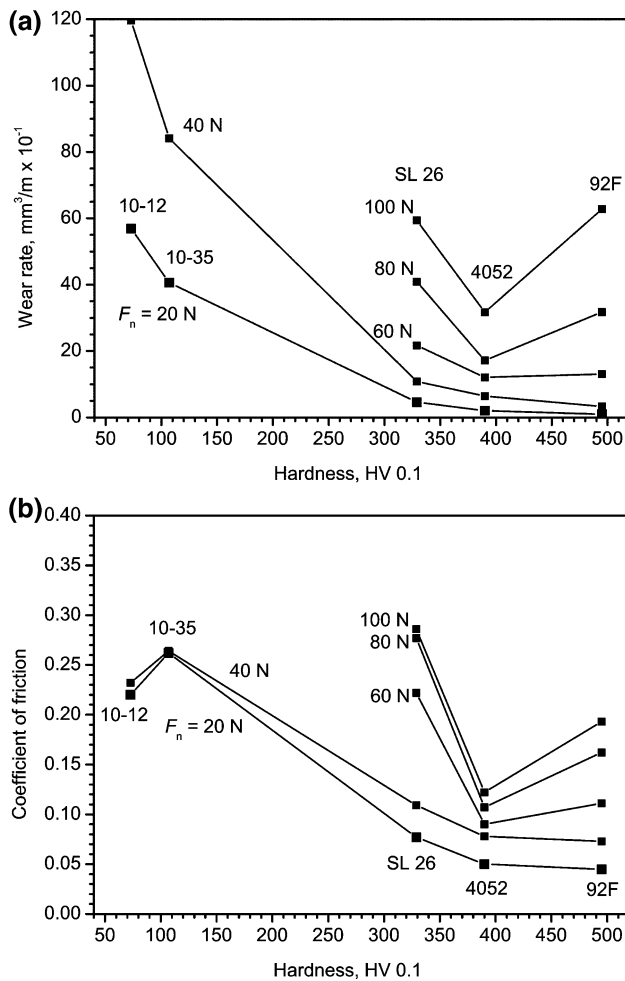


Fig. 11 Relationship between: **a** wear rate and hardness and **b** coefficient of friction and hardness, for the scratch testing (for all tested materials)

In the scratch testing, there was a correlation between wear rate and friction coefficient values for coatings, i.e. lower coefficients of friction implies lower wear rates, while for composites there were reversed effect, i.e. lower coefficients of friction implies higher wear rates (Fig. 11). Completely different situation was in the pin-on-disc testing where there was a correlation between wear rate and friction coefficient values for composites, i.e. lower coefficients of friction implies lower wear rates, while for coatings there were reversed effect, i.e. lower coefficients of friction implies higher wear rates (Fig. 12).

For better comparison of the two abrasion tests, relationships of wear and friction results from these tests were presented, in the form of diagrams, on Figs. 13 and 14. Since five different loads were applied in the scratch testing, a wear factor, i.e. a specific wear rate parameter was used to make a comparison. Wear factors of the tested materials were calculated from the following equation:

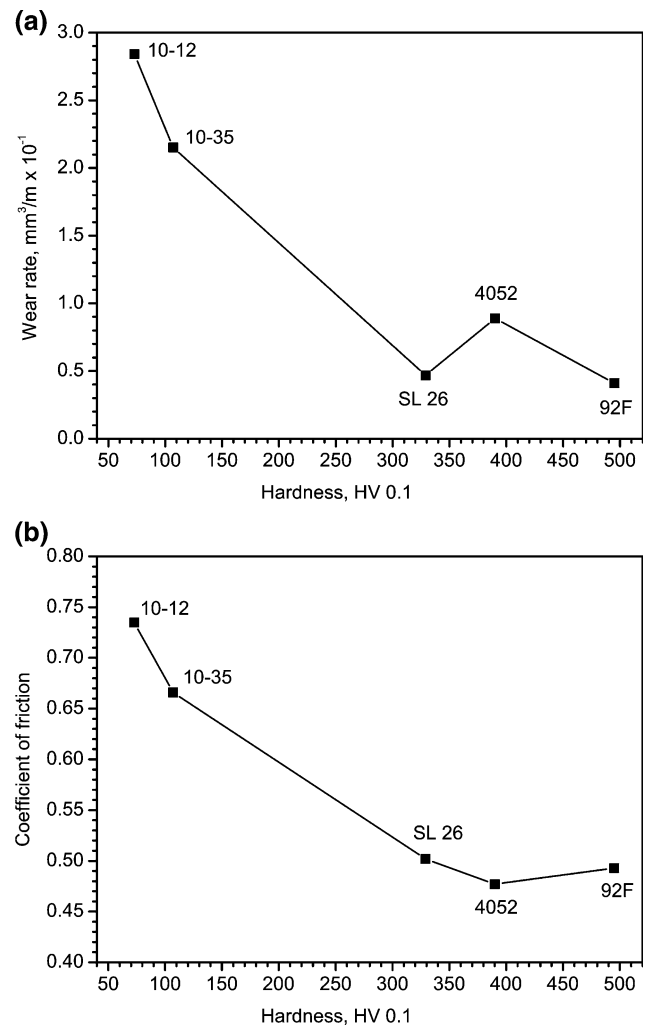


Fig. 12 Relationship between: **a** wear rate and hardness and **b** coefficient of friction and hardness, for the pin-on-disc testing (for all tested materials)

$$V = K \cdot F \cdot s$$

where V is wear volume in mm³, K is wear factor in mm³/Nm, F is normal load in N and s is sliding distance in m. In this way, by using the wear factor parameter, the influence of normal load is eliminated.

In scratch testing, there is only one abrasive particle (indenter) in contact with the tested material, while in pin-on-disc testing there were a lot of particles in contact. Using the wear factor parameter, the influence of the number of particles in contact is also diminished. If it is assumed that there is n_p number of particles of abrasive paper in contact with the tested material, then the total wear volume (V) will be the wear volume produced by one particle (V_i) multiplied by n_p . The total normal load (F) will be the normal load acting on one particle in contact (F_i) multiplied by n_p . The previous equation will then become:

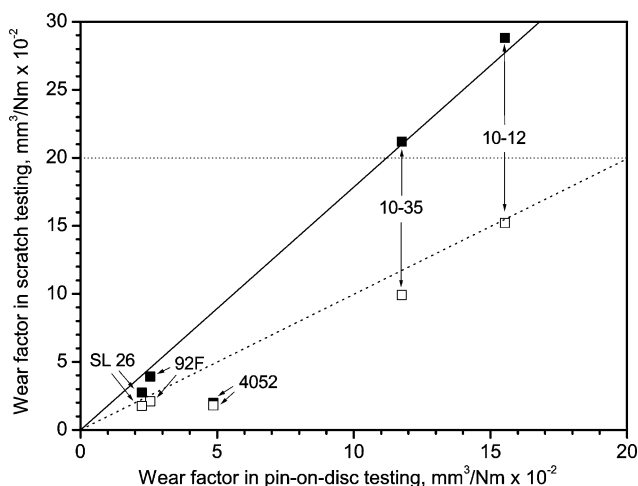


Fig. 13 Wear factor mean values in scratch testing as a function of wear factor in pin-on-disc testing (*closed square* symbols are for first method of calculation whereas *open square* symbols are for second method of calculation)

$$V_i \cdot n_p = K \cdot F_i \cdot n_p \cdot s$$

from which it could be seen that the number of particles (n_p) does not influence the wear factor value on the macro scale.

In order to try to eliminate the influence of plastic deformation of some tested materials, a second method of wear volume calculation for scratch testing was also applied. In the first method, as it was described previously, the volume loss was calculated from the cross-sectional area of displaced material (A_D , Fig. 2), multiplied by the wear track length. The second method comprises a thesis adopted by Sinha et al. [42] that the worn material is actually the material detached from the bulk material, so in the second method the volume loss was calculated from the difference of cross-sectional area of displaced material and

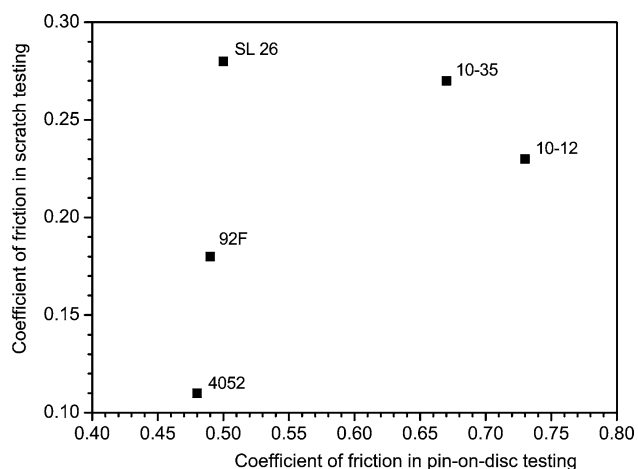


Fig. 14 Coefficient of friction in scratch testing as a function of coefficient of friction in pin-on-disc testing

cross-sectional area of formed ridges ($A_D - A_R$, Fig. 2), multiplied by the wear track length.

Wear factors for composite materials did not vary a lot with normal load and had approximately the same values for all applied loads. For SL 26 and both coatings wear factors showed a tendency of grow with increase of normal load. This implies a change of dominant mechanism of wear. Nevertheless, the mean values of the wear factors for these materials were also adopted as adequate for comparison. All obtained values of wear factors were in expected range for abrasive wear.

Relationship between wear factors from two abrasion tests is more or less linear, with the exception of coating 4052 (Fig. 13). This is principally because of the different contact geometry between these two tests and the fact that scratch test was a single-pass test while pin-on-disc was more like multiple-pass scratch test. Repeated action of the abrasives (in pin-on-disc test) forced the detachments of the whole coatings parts, which was more intensive for coating 4052 due to the higher presence of oxides and pores. Application of the second method of wear volume calculation in scratch testing gives slightly better correlation with pin-on-disc testing, but exception of coating 4052 is still present. Obtained results show that, to some extensions, scratch tester can be used for determination of abrasive wear resistance. On the other hand, there is very little if any correlation between the coefficients of friction obtained from two different abrasion tests (Fig. 14).

5 Conclusions

The idea of this research was to determine abrasion wear behaviour of five different materials (grey cast iron, two ferrous-based coatings and two aluminium-based composites with Al_2O_3 reinforcements) alongside with the investigation of the possibility of the abrasive wear resistance determination with scratch tester.

Microstructures, hardness and tribological properties of the tested materials were investigated and concluded that both coatings, from the aspect of abrasive wear, could be an adequate substitution for the grey cast iron, while both composites showed poor abrasive wear properties (especially in high-load conditions) comparing with grey cast iron.

The abrasive wear results of both tests used in this study indicate that a general trend is valid, namely, a higher hardness is usually associated to a better resistance to abrasion and lower coefficient of friction. It was also confirmed that for this type of materials the hardness is not the best property for predicting of the abrasive wear behaviour, since it is not necessary that the material with the highest hardness have the highest abrasive wear resistance.

In both abrasion wear tests, there was more than one exception from the general trend, which implies that the investigated material was not homogeneous enough. On the other hand, both tests showed that they could be used for ranking of various materials and in discerning of its wear mechanisms. A clear correlation and functional relationship between data from these two abrasion wear tests did not emerge. However, a trend within classes of alloys was present, and good/poor performers was stand out.

Finally, scratch test offers relatively easy and quick comparison of different materials on abrasive wear, with good repeatability of the results, and although the wear rate in a scratch test does not necessarily describe the wear rate in a real application, because of its simplicity and idealization, it provides some fundamental evidence for the abrasive wear phenomenon.

References

- Rac, A.: Basics of Tribology, Faculty of Mechanical Engineering, University of Belgrade, Belgrade (1991)
- Tucker Jr., R.C.: Wear failures. In: Metals Handbook. Failure Analysis and Prevention, vol. 11, pp. 154–162, 9th edn. American Society for Metals, Metals Park (1986)
- Gates, J.D.: Two-body and three-body abrasion: a critical discussion. *Wear* **214**, 139–146 (1998)
- Abrasive wear resistance. *Ind. Lubr. Tribol.* **43**, 14–26 (1991)
- ASTM G 65-04 Standard Test Method for Measuring Abrasion Using the Dry Sand/Rubber Wheel Apparatus (2004)
- ASTM G 81-97a Standard Test Method for Jaw Crusher Gouging Abrasion Test (2007)
- ASTM G 105-02 Standard Test Method for Conducting Wet Sand/Rubber Wheel Abrasion Tests (2007)
- ASTM G 132-96 Standard Test Method for Pin Abrasion Testing (2007)
- ASTM G 174-04 Standard Test Method for Measuring Abrasion Resistance of Materials by Abrasive Loop Contact (2004)
- Hawk, J.A., Wilson, R.D., Tylczak, J.H., Doğan, Ö.N.: Laboratory abrasive wear tests: investigation of test methods and alloy correlation. *Wear* **225–229**, 1031–1042 (1999)
- Sinha, S.K.: 180 years of scratch testing. *Tribol. Int.* **39**, 61 (2006)
- Bull, S.J., Berasetegui, E.G.: An overview of the potential of quantitative coating adhesion measurement by scratch testing. *Tribol. Int.* **39**, 99–114 (2006)
- EN 1071-3:2002 Advanced Technical Ceramics—Methods of Test for Ceramic Coatings—Part 3: Determination of Adhesive and Other Mechanical Failure Modes by a Scratch Test (2002)
- Williams, J.A.: Analytical models of scratch hardness. *Tribol. Int.* **29**, 675–694 (1996)
- Bull, S.J.: Can scratch testing be used as a model for the abrasive wear of hard coatings? *Wear* **233–235**, 412–423 (1999)
- Xie, Y., Hawthorne, H.M.: The damage mechanisms of several plasma-sprayed ceramic coatings in controlled scratching. *Wear* **233–235**, 293–305 (1999)
- Xie, Y., Hawthorne, H.M.: Wear mechanism of plasma-sprayed alumina coating in sliding contacts with harder asperities. *Wear* **225–229**, 90–103 (1999)
- Zhang, Z.F., Zhang, L.C., Mai, Y.-W.: Particle effects on friction and wear of aluminium matrix composites. *J. Mater. Sci.* **30**, 5999–6004 (1995)
- Sinha, S.K., Reddy, S.U., Gupta, M.: Scratch hardness and mechanical property correlation for Mg/SiC and Mg/SiC/Ti metal-matrix composites. *Tribol. Int.* **39**, 184–189 (2006)
- Gee, M.G.: Low load multiple scratch tests of ceramics and hard metals. *Wear* **250**, 264–281 (2001)
- Vencl, A., Mrdak, M., Cvijović, I.: Microstructures and tribological properties of ferrous coatings deposited by APS (Atmospheric Plasma Spraying) on Al-alloy substrate. *FME Trans.* **34**, 151–157 (2006)
- Mišković, Z., Bobić, I., Tripković, S., Rac, A., Vencl, A.: The structure and mechanical properties of an aluminium A356 alloy base composite with Al₂O₃ particle additions (MMC). *Tribol. Ind.* **28**, 23–27 (2006)
- Standard Practices Manual (PN 582005) Turbojet Engine. Pratt & Whitney, East Hartford (2002)
- ASTM C 633-01 Standard Test Method for Adhesion or Cohesion Strength of Thermal Spray Coatings (2001)
- Hwang, B., Ahn, J., Lee, S.: Correlation of microstructure and wear resistance of ferrous coatings fabricated by atmospheric plasma spraying. *Metall. Mater. Trans. A* **33A**, 2933–2945 (2002)
- Schorr, B.S., Stein, K.J., Marder, A.R.: Characterization of thermal spray coatings. *Mater. Charact.* **42**, 93–100 (1999)
- Edrisi, A., Perry, T., Cheng, Y.T., Alpas, A.T.: The effect of humidity on the sliding wear of plasma transfer wire arc thermal sprayed low carbon steel coatings. *Surf. Coat. Technol.* **146–147**, 571–577 (2001)
- Technical Bulletin Metco® 92F High Carbon Iron Powder. Metco Inc., New York (1975)
- Barbezat, G., Schmid, J.: Plasmabeschichtungen von zylinderkurbelgehäusen und ihre bearbeitung durch honen. *MTZ* **62**, 314–320 (2001)
- Li, R.X., Li, R.D., Zhao, Y.H., He, L.Z., Li, C.X., Guan, H.R., Hu, Z.Q.: Age-hardening behavior of cast Al–Si base alloy. *Mater. Lett.* **58**, 2096–2101 (2004)
- Prchlik, L., Sampath, S.: Effect of the microstructure of thermally sprayed coatings on friction and wear response under lubricated and dry sliding conditions. *Wear* **262**, 11–23 (2007)
- Hwang, B., Lee, S., Ahn, J.: Effect of oxides on wear resistance and surface roughness of ferrous coated layers fabricated by atmospheric plasma spraying. *Mater. Sci. Eng. A* **335**, 268–280 (2002)
- Rabiei, A., Mumm, D.R., Hutchinson, J.W., Schweinfest, R., Rühle, M., Evans, A.G.: Microstructure, deformation and cracking characteristics of thermal spray ferrous coatings. *Mater. Sci. Eng. A* **269**, 152–165 (1999)
- Garcia-Cordovilla, C., Narciso, J., Louis, E.: Abrasive wear resistance of aluminium alloy/ceramic particulate composites. *Wear* **192**, 170–177 (1996)
- Al-Rubaie, K.S.: Abrasive wear of Al–SiC composites. *Materi- alwissenschaft und Werkstofftechnik* **31**, 300–311 (2000)
- Vencl, A., Rac, A., Marinković, A.: Tribological properties of ferrous-based coatings deposited by APS on Al-alloy substrate under dry sliding conditions. In: Proceedings of the 6th International Conference on Tribology—BALKANTRIB'08, p. 149. Technical University, Sofia (2008)
- Vencl, A., Bobić, I.: Tribological properties of A356 Al–Si alloy base composite reinforced with Al₂O₃ particles (MMC). In: Proceedings of the 5th Congress of the Metallurgists of Macedonia, p. 122. Macedonian Metallurgists union, Skopje (2008)
- Khrushov, M.M.: Resistance of metals to wear by abrasion, as related to hardness. In: Proceedings of the International

- Conference on Lubrication and Wear, pp. 654–658. Institute of Mechanical Engineers, London (1957)
39. Khrushov, M.M.: Principles of abrasive wear. *Wear* **28**, 69–88 (1974)
 40. Sundararajan, G.: The differential effect of the hardness of metallic materials on their erosion and abrasion resistance. *Wear* **162–164**, 773–781 (1993)
 41. Straffelini, G., Bonollo, F., Molinari, A., Tiziani, A.: Influence of matrix hardness on the dry sliding behaviour of 20 vol. % Al_2O_3 -particulate-reinforced 6061 Al metal matrix composite. *Wear* **211**, 192–197 (1997)
 42. Sinha, S.K., Chong, W.L.M., Lim, S.-C.: Scratching of polymers—Modelling abrasive wear. *Wear* **262**, 1038–1047 (2007)